3D MHD simulations of runaway electron avalanche in ITER mitigated disruptions

C. Wang[a], M. Kong[a], J. P. Graves[a], F. J. Artola[b], E. Nardon[c], M. Hoelzl[d], the JOREK team[e]

[a] *École Polytechnique Fédérale de Lausanne (EPFL), Swiss Plasma Center (SPC), CH-1015 Lausanne, Switzerland*
[b] *ITER Organization, Route de Vinon-sur-Verdon, 13115 Saint-Paul-lez-Durance, France*
[c] *IRFM, CEA Cadarache, 13108 Saint-Paul-lez-Durance, France*
[d] *Max Planck Institute for Plasma Physics, Boltzmannstr. 2, 85748 Garching b. M., Germany*
[e] *See the author list of M. Hoelzl et al, 2024 Nucl. Fusion 64 112016*

1. Introduction

Disruptions are the rapid termination of tokamak discharges [1], usually composed of a rapid thermal quench (TQ) and a subsequent current quench (CQ). During the CQ, the remaining plasma current I_p induces a strong loop electric field in the cold and resistive plasma. The preexisting high-energy electrons, which are called the runaway electron (RE) seeds [2], can be accelerated by this electric field to relativistic speed and become REs. The knock-on collisions between REs and thermal electrons lead to an exponential avalanche of RE population:

$$I_{RE} = I_{seed} \cdot e^{\Delta I_p / I_c} \equiv I_{seed} \cdot g_{RE} \tag{1}$$

where I_{RE} is the current carried by the REs, I_{seed} is the seed current, $\Delta I_p / I_c$ is the normalized decay of the plasma current, and g_{RE} is the avalanche gain. Due to the high plasma current on ITER (up to 15 MA), the avalanche of REs could potentially generate several megaamperes of RE current during the CQ [3], which might damage the plasma-facing components. Previous studies have suggested that keeping I_{RE} below the safe limit of 150 kA would be difficult on ITER [4], especially in D-T operations where tritium and activated wall material provide extra nuclear seeds. However, before the number of REs increases to a large value, some REs might be lost due to magnetic stochasticity caused by the growth of MHD instabilities, such as tearing modes [5; 6]. In our work, MHD-induced RE loss is estimated in CQ simulations using the JOREK code, which employs a 3D reduced MHD model self-consistently coupled to a fluid description of REs. Tracing particles of REs are used to evaluate their precise transport.

2. Current density profile and MHD stability

The stability of the tearing modes is primarily determined by the current density profile of the plasma. Considering the uncertainty of the current distribution in the post-TQ plasma, we conduct a scan of different current profiles to investigate their stability in CQ. The most

stable and most unstable cases will be selected for more detailed CQ simulations as the worst-case and best-case scenarios regarding RE mitigation.

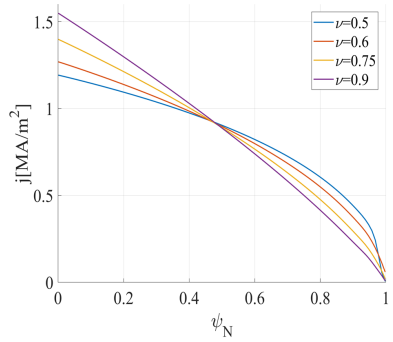

Figure 1: j profiles used in the scan.

In the scan, we use a simplified JOREK model and run the simulations until the MHD mode energies grow from the noise level to saturation. Three toroidal harmonics n=1-3 are included in these 3D simulations. The starting point of the CQ simulation is based on the ITER scenario after disruption mitigation. The density and temperature profiles are fixed to $n_e = 5 \times 10^{20}$ m^{-3} and $T_e = T_i = 10$ eV on the axis. The toroidal magnetic field $B_0 = 5.3$ T and the initial plasma current $I_p = 15$ MA. The initial j profiles are taken from the following function of the normalized poloidal magnetic flux ψ_N with one parameter ν that we will scan over and one coefficient j_0 to conserve the magnetic helicity: [7]

$$j = j_0(1 - \psi_N)^\nu \tag{2}$$

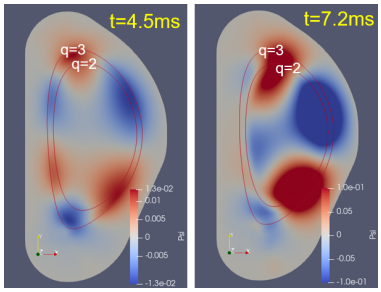

Figure 2: $n = 1$ component of poloidal magnetic flux ψ under the $\nu = 0.5$ current profile.

As shown in Fig.1, a larger ν gives a peaked j profile, while a smaller ν makes it flatter. In the stability scan, most MHD modes show higher growth rates and usually result in global magnetic stochasticity under flatter current profiles ($\nu \leq 0.75$). In contrast, MHD activities are milder and closed FSs survive longer under peaked j profiles. The dominant instabilities here are tearing modes driven by the current gradient. A flat current density profile in the plasma center leaves a steep edge where a high current density gradient drives the tearing modes on the edge FSs with rational safety factor q, e.g., $q = 3$ and $q = 5/2$ surfaces. The growth of these modes perturbs the inner rational FSs (Fig.2) and triggers instabilities there. Eventually, overlapped modes lead to global magnetic stochasticity and destroy all FSs.

3. RE deconfinement during CQ

In this section, more realistic CQ simulations are performed based on two typical initial j profiles: a stable one and an unstable one. According to the result in the previous section, a peaked j profile (Case 1 in Fig.3) is used as the worst-case scenario, where MHD activity is relatively mild and REs can be well confined over a longer time scale. A flat profile (Case 2 in Fig.3) acts as an unstable reference, where the REs are expected to be rapidly deconfined by magnetic stochasticity. In disruption events on present tokamaks, an I_p spike is usually observed in the plasma current waveform during TQ [8], which indicates the flattening of the

j profile due to magnetic reconnection. Therefore, Case 2 is assumed to be a more realistic post-TQ scenario.

The initial condition of the simulation is still based on the ITER plasma after mitigation injection and TQ, where $n_H = 3.9 \times 10^{20}$ m^{-3} and $n_{Ne} = 6.1 \times 10^{18}$ m^{-3} uniformly. The temperature is calculated from the balance between Ohmic heating and impurity radiation. REs are described by a fluid model [9] coupled with the MHD model. $I_{seed} = 10$ mA at the beginning of CQ as a typical value of nuclear seeds in ITER D-T operations. The RE avalanche is well reproduced in this model, while the RE transport is over-simplified. Considering the huge computational resources required to simulate the RE advection at the speed of light along the stochastic field, the parallel transport of REs is represented by a diffusion model with $D_{RE,\parallel} = 1.54 \times 10^6$ m^2/s. Therefore, RE loss from magnetic stochasticity will be underestimated in this model. The realistic RE deconfinement will be evaluated by particle tracing at several time points, while I_{RE} from the RE fluid model will be used as a reference to determine whether the deconfinement occurs sufficiently early under a small I_{RE}.

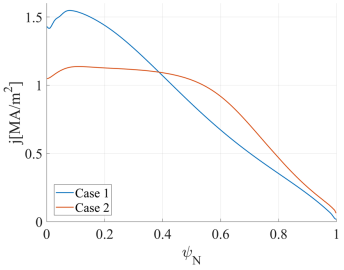

Figure 3: j profiles for Case 1 and Case 2.

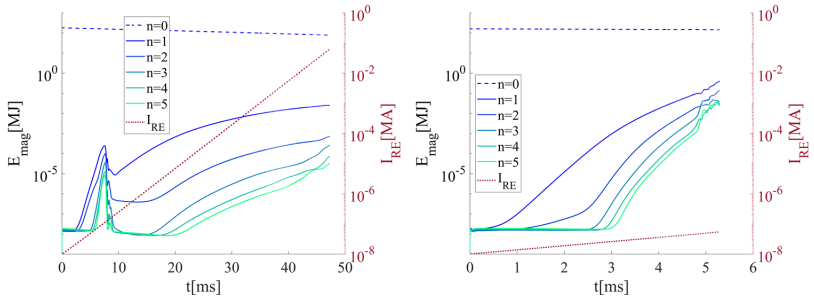

(a) Case 1 (b) Case 2

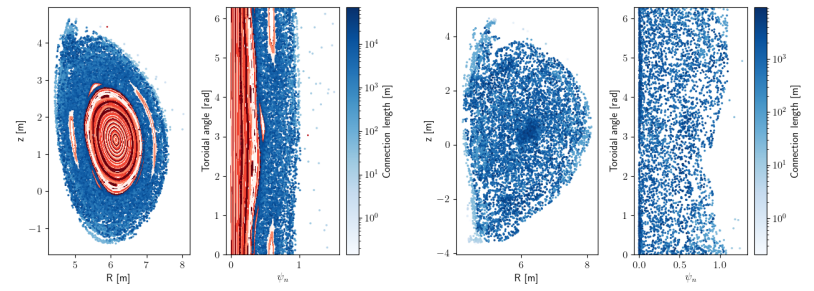

(c) Case 1, t=48.5 ms (d) Case 2, t=5.3 ms

Figure 4: (a),(b): Mode energy evolution and I_{RE} growth. (c),(d): The Poincaré plots from particle tracing of 10MeV REs with a pitch angle of 0.99. The connection length is the distance a RE needs to travel before reaching the wall.

These two simulations both include five toroidal harmonics. The evolution of their magnetic energies and the reference I_{RE} from RE fluid are shown in Fig.4a,4b. The initial energies may be different in real post-TQ plasma. In Case 1, all modes grow rather slowly after the E_{mag} spike (∼8 ms) from the 1/1 kink mode. The Poincaré plot from particle tracing of 10MeV REs is given in Fig.4c when the fluid $I_{RE} =$ 100 kA is close to the safe limit of 150 kA. Although a growing 2/1 tearing mode has destroyed more than

half of the FSs, the core FSs are still closed. Because of the higher toroidal electric field in the central plasma, most REs are generated in this confined region. An MA-level RE beam is expected to be generated in Case 1 if the core FSs stay closed for another 10 ms. However, as the RE current density gets comparable to the Ohmic one, its influence on MHD becomes non-negligible. A more realistic RE transport model is required to simulate the rest of the CQ with RE-MHD coupling. In Case 2, as expected, the mode energies grow much faster (Fig.4b) and global magnetic stochasticity is achieved within 5 ms. According to the Poincaré plot in Fig.4d, no confined region exists after 5.3 ms. All tracing REs have a connection length to the wall shorter than 10^4 m, meaning that they will all get deconfined within 0.03 ms. Although this deconfinement event would certainly reduce the risk of REs, some FSs could heal after global magnetic reconnection. Then REs might re-avalanche from the nuclear seeds. Further simulation of Case 2 to the end of CQ is ongoing, but numerical issues in the presence of the drastic magnetic reconnection add difficulties to this work.

4. Conclusions and outlook

The MHD evolution and RE deconfinement by magnetic stochasticity during the CQ in ITER are modeled using 3D JOREK simulations under various initial current density profiles. Edge current gradient is found to play an essential role in triggering large-scale tearing modes and the ensuing magnetic stochasticity. REs are expected to be partially or completely lost in this reconnection event. Together with other mechanisms such as the scraping-off effect and optimized mitigation injection, even temporary or partial deconfinement could potentially facilitate the RE avoidance on ITER. To investigate whether the REs will re-avalanche after some FSs recover and how much the final I_{RE} would be, further simulations until the end of the CQ with an improved RE fluid transport model are required. In addition, a more realistic post-TQ plasma scenario from corresponding TQ simulations will be applied to future CQ simulations.

This work has been carried out within the framework of the EUROfusion Consortium, partially funded by the European Union via the Euratom Research and Training Programme (Grant Agreement No 101052200 — EUROfusion). The Swiss contribution to this work has been funded by the Swiss State Secretariat for Education, Research and Innovation (SERI). Views and opinions expressed are however those of the author(s) only and do not necessarily reflect those of the European Union, the European Commission or SERI. Neither the European Union nor the European Commission nor SERI can be held responsible for them. This work was supported in part by the Swiss National Science Foundation. The views and opinions expressed herein do not necessarily reflect those of the ITER Organization.

References

[1] A.H. Boozer, Phys. Plasmas **19**, 2012
[2] J.R. Martín-Solís et al, Nucl. Fusion **57**, 2017
[3] A.H. Boozer, Phys. Plasmas **22**, 2015
[4] O. Vallhagen et al, Nucl. Fusion **64**, 2024
[5] F.J. Artola et al, Nucl. Fusion **62**, 2022
[6] L. Carbajal et al, Phys. Plasmas **27**, 2020
[7] J. Wesson et al, *Tokamaks*, 2004
[8] S. Zeng et al, Phys. Plasmas **30**, 2023
[9] V. Bandaru et al, Phys. Rev. **99**, 2019